

RESEARCH ARTICLE

Acid sphingomyelinase deficiency enhances myelin repair after acute and chronic demyelination

Marwan Chami^{1*}, Ramona Halmer¹, Laura Schnoeder¹, Katrin Anne Becker², Carola Meier³, Klaus Fassbender¹, Erich Gulbins^{2,4}, Silke Walter^{1,5,6}

1 Department of Neurology, Saarland University Hospital, Homburg, Germany, **2** Department of Molecular Biology, University Hospital Essen, University of Duisburg-Essen, Essen, Germany, **3** Institute of Anatomy and Cell Biology, Saarland University, Homburg, Germany, **4** Department of Surgery, University of Cincinnati, Cincinnati, Ohio, United States of America, **5** Department of Medicine, Royal Melbourne Hospital, University of Melbourne, Parkville, Victoria, Australia, **6** Florey Institute of Neuroscience and Mental Health, University of Melbourne, Parkville, Victoria, Australia

* Marwan.chami@uniklinikum-saarland.de



OPEN ACCESS

Citation: Chami M, Halmer R, Schnoeder L, Anne Becker K, Meier C, Fassbender K, et al. (2017) Acid sphingomyelinase deficiency enhances myelin repair after acute and chronic demyelination. *PLoS ONE* 12(6): e0178622. <https://doi.org/10.1371/journal.pone.0178622>

Editor: Martin Stangel, Hannover Medical School, GERMANY

Received: February 13, 2017

Accepted: May 16, 2017

Published: June 5, 2017

Copyright: © 2017 Chami et al. This is an open access article distributed under the terms of the [Creative Commons Attribution License](https://creativecommons.org/licenses/by/4.0/), which permits unrestricted use, distribution, and reproduction in any medium, provided the original author and source are credited.

Data Availability Statement: All relevant data are within the manuscript and figures.

Funding: Support was provided by Deutsche Forschungsgemeinschaft (DFG) German Research Foundation: Priority Program 1267 [http://www.dfg.de/foerderung/info_wissenschaft/2009/info_wissenschaft_09_54/index.html] to EG and SW. The funders had no role in study design, data collection and analysis, decision to publish, or preparation of the manuscript.

Abstract

The cuprizone animal model, also known as the toxic demyelination model, is a well-reproducible model of demyelination- and remyelination in mice, and has been useful in studying important aspect of human demyelinating diseases, including multiple sclerosis. In this study, we investigated the role of acid sphingomyelinase in demyelination and myelin repair by inducing acute and chronic demyelination with 5- or 12-week cuprizone treatment, followed by a 2-week cuprizone withdrawal phase to allow myelin repair. Sphingolipids, in particular ceramide and the enzyme acid sphingomyelinase, which generates ceramide from sphingomyelin, seem to be involved in astrocyte activation and neuronal damage in multiple sclerosis. We used immunohistochemistry to study glial reaction and oligodendrocyte distribution in acid sphingomyelinase deficient mice and wild-type C57BL/6J littermates at various time intervals after demyelination and remyelination. Axonal injury was quantified using amyloid precursor protein and synaptophysin, and gene expression and protein levels were measured using gene analysis and Western blotting, respectively. Our results show that mice lacking acid sphingomyelinase had a significant increase in myelin recovery and a significantly higher oligodendrocyte cell count after 2 weeks remyelination compared to wild-type littermates. Detrimental astroglial distribution was also significantly reduced in acid sphingomyelinase deficient animals. We obtained similar results in experiments using amitriptyline to inhibit acid sphingomyelinase. These findings suggest that acid sphingomyelinase plays a significant role in myelin repair, and its inhibition by amitriptyline may constitute a novel therapeutic approach for multiple sclerosis patients.

Competing interests: The authors have declared that no competing interests exist.

Introduction

Demyelination is a key feature of multiple sclerosis (MS), an autoimmune disease that is the main cause of permanent disability in young adults. [1] Histopathologically, MS is associated with the widespread presence of demyelinated plaques, ultimately leading to oligodendrocyte loss and neurodegeneration. Depending on the disease stage, mechanisms that are associated with demyelination in MS include, among others, invasion of auto-aggressive leukocytes, toxic accumulation of oligodendrocyte-released iron, oxidative stress, mitochondrial injury and microglial activation. [2] These mechanisms activate astrocytes, which appear to play both beneficial and detrimental roles in MS disease progression. [3, 4, 5, 6, 7] To date, there are no therapeutic options to control demyelination in MS, nor treatments to repair myelin damage sufficiently in chronic MS.

CNS demyelination can be investigated by treatment with cuprizone (*bis-cyclohexanone oxaldihydrazone*), a toxic copper-chelating agent. In animal models, cuprizone treatment, is a standard method for inducing demyelination as part of the chronic phase of multiple sclerosis, resulting in astrocyte activation [8] and strong demyelination with oligodendrocyte cell death in distinct brain areas, but not in spinal cord. Myelin recovery can occur after cuprizone withdrawal, making the cuprizone model useful for investigating both acute demyelination and myelin repair mechanisms.

Acid sphingomyelinase (Asm), a lysosomal enzyme, hydrolyses the membrane lipid sphingomyelin into ceramide. [9, 10, 11, 12] A recent study demonstrated increased Asm activity in astrocytes in active MS lesions. [13] Other studies have shown ceramide to be important in the regulation and induction of oligodendrocyte cell death in human MS brains. [14]

Asm/ceramide may play a regulatory role in MS pathogenesis; investigation of their role may support the development of novel therapeutic strategies. To investigate the role of the Asm/ceramide system in demyelination, we examined the effects of genetic deficiency or pharmacological inhibition of Asm on the pathophysiological features of remyelination in the cuprizone-treatment animal model.

Materials and methods

Animals

All animal experiments were approved by the Ethical Review Committee of the Regional Council in Saarland, Germany. *In vivo* experiments were performed with 8-week-old male acid sphingomyelinase deficient mice (*Asm*^{-/-}; protein: Asm, gene symbol: *Smpd1*) and wild-type (C57BL/6J) littermates obtained from our breeding facility. All mice were maintained in a pathogen-free environment; food and water were available *ad libitum*.

Cuprizone-induced demyelination and amitriptyline treatment

Mice were fed with powdered food supplemented with 0.2% cuprizone (*bis-cyclohexanone-oxaldihydrazone*, Sigma-Aldrich, St. Louis, MO, USA) for 5 weeks (acute demyelination) or for 12 weeks (chronic demyelination). Afterwards, animals were fed with normal diet for the following 2 weeks to allow remyelination as previously shown. [8] Pharmacological Asm inhibition was achieved during the 2-week-recovery phase by twice daily intraperitoneal injections with 25 mg/kg amitriptyline dissolved in sterile distilled water, to insure the drug's full function as previously described. [15] PBS injections were administered as control. The twice-daily dosing schedule was chosen to maintain a constant plasma level of amitriptyline as described earlier. [15] Animals subjected to a cuprizone-free diet served as untreated (naïve) controls; additional controls were animals given a cuprizone-free diet who received amitriptyline

treatment. To evaluate amitriptyline's effect in non-demyelinating conditions, amitriptyline-injected mice were compared to naïve controls.

Immunohistochemistry

For immunohistochemical analysis, animals were sacrificed by isoflurane inhalation (Abbott, Wiesbaden Germany), perfused with ice-cold phosphate-buffered saline (pH 7.4, PBS, Sigma-Aldrich, Steinheim, Germany) followed by 4% paraformaldehyde (PFA, Sigma-Aldrich). Brains were post-fixed in 4% PFA overnight. Thereafter, brains were paraffin-embedded and processed into 5 μ m coronal sections between bregma-0.82mm and bregma -1.82mm according to the mouse atlas.[16] Sections were placed on silane-coated slides, de-paraffinized, re-hydrated and heat-unmasked using citrate buffer, pH 6.0, with 3 times 5 minutes microwave cooking at 600W. Slides were treated with 3% H₂O₂ (Roth, Karlsruhe, Germany) diluted in PBS/17% methanol for 30 minutes to block endogenous peroxidase, followed by 1-hour treatment with 0.2% Casein (w/v; Sigma-Aldrich) + 0.1% Tween 20 (Sigma-Aldrich) + 0.1% Triton X-100 (Sigma-Aldrich) diluted in PBS for 1-hour. Afterwards, sections were exposed overnight at 4°C to the following primary antibodies diluted in blocking buffer: rabbit polyclonal anti-Iba-1 (1:200, Wako, Neuss, Germany), mouse monoclonal anti-synaptophysin (1:50, ab8049, Abcam, Cambridge, UK), rabbit polyclonal anti-Olig-2 (1:1000, ab8109, Abcam), rabbit polyclonal anti-myelin basic protein (MBP) (1:500, ab40390, Abcam), rabbit polyclonal anti-amyloid precursor protein (APP) (1:1000, a8717, Sigma-Aldrich, St. Louis, USA), rat monoclonal anti-glial fibrillary acidic protein (GFAP) (1:1000, 13-0300, Invitrogen, Darmstadt, Germany). The next day, sections were incubated with the appropriate secondary antibodies: biotin SP conjugated goat anti-mouse (1:500, ab128976, Abcam), biotin SP conjugated goat anti-rabbit (1:300, Jackson immune research laboratories, Baltimore, USA) or goat anti-rabbit *Alexa-Fluor*[®]-488 conjugate (1:500, 1670152, Invitrogen, Rockford, USA) for 1 hour at room temperature. Slides were developed using the Vectastain elite ABC kit (PK-6104, rat IgG, Vector laboratories, Burlingame CA, USA) applied according to the manufacturer's recommendations. Diaminobenzidine (DAB, Sigma-Aldrich) was used as chromogen, at 1 mg/ml in PBS. Finally, sections were counter stained with hematoxylin for 30 seconds, dehydrated in graded alcohols if required and mounted with Entellan[®] (Merck, Darmstadt, Germany) or Moviol (Roth, Karlsruhe, Germany).

Quantification of glial cells and axonal degeneration

Quantification of oligodendrocyte, microglia, astrocyte cell counts, synaptophysin and APP positive bulbs was performed by manually counting the number of positive structures in the medial corpus callosum (CCm). For each animal 2–3 slides were analyzed with a distance of 150 μ m in between. Cell counts were averaged for each animal and the mean was calculated for each experimental group. All studies were performed at an AxioImager Z2 microscope (Zeiss, Jena, Germany), 20x or 40x lens. Cell numbers are expressed as cells per mm². As an additional parameter for astrogliosis and microgliosis, the surface area covered by GFAP and Iba-1 staining was determined using a densitometric scanning procedure (ImageJ software, Maryland, USA). Results are expressed as relative GFAP or Iba-1 covered area of the CCm (percentage of the stained area in relation to the non-stained area) as previously described. [17]

Determination of de- and remyelination

The extent of de- and remyelination in the corpus callosum was examined by staining coronal brain sections of CCm with luxol fast blue (LFB, RAL diagnostics, Martillac, France) and

periodic acid-Schiff (PAS) (Merck, Darmstadt, Germany). Sections were graded on a scale from 0 (complete demyelination) to 3 (normal myelin). [18] Anti-myelin basic protein staining was performed as described above to quantify the fluorescence intensity of myelin in the CCm (ImageJ).

RNA isolation and real-time PCR

The CCm was dissected from whole brains under a light microscope. Total RNA was then extracted from the tissue with Trizol (Life Technologies, Ober-Olm, Germany). First-strand cDNA was synthesized by priming total RNA with hexamer random primers (Life Technologies) and using Superscript III reverse transcriptase (Life Technologies). For quantification of gene transcripts, real-time PCR was performed with SYBR green (Roche Applied Science, Mannheim, Germany) using a 7500 Fast Real-Time PCR System (Life Technologies). The amount of double-stranded PCR product synthesized in each cycle was measured by detecting the FAM dye freed from the SYBR green, which binds to double-stranded DNA. Threshold cycle (Ct) values for each test gene from the replicate PCRs were normalized to the Ct values for *gapdh* control from the same cDNA preparations. Transcription ratios were calculated as $2^{(\Delta Ct)}$ where ΔCt is the difference between Ct (*gapdh*) and Ct (test gene). Table 1 lists the primers used and the genes analyzed.

SDS-PAGE and Western blot

Myelin oligodendrocyte glycoprotein (MOG) levels were analyzed using Western blotting. The CCm was dissected from whole brains under a light microscope and bounce-homogenized in a Tris-buffered saline (TBS) solution containing a protease inhibitor cocktail (Roche Applied Science, Mannheim, Germany). Protein concentration was measured using the Bradford assay (Bio-Rad, München, Germany) according to the manufacturer's protocol. Equal amounts of protein samples were separated by 12% discontinuous sodium dodecyl sulphate-polyacrylamide gel electrophoresis (SDS-PAGE), and transferred onto PVDF membranes (Roche Applied Science, Mannheim, Germany). Membranes were then blocked for 1 hour at room temperature using 10% nonfat dry milk dissolved in PBS. After the 1 hour blocking, PVDF membranes were incubated with mouse anti-MOG (1:2000, MAB5680, Millipore, Darmstadt, Germany) over night at 4°C. Next day, membranes were washed for 30 minutes using Tris-buffered saline containing 0.05% Tween 20 (TBS-T) and were incubated with a peroxidase-conjugated goat anti-mouse (1:3000, P0447, Dako, Hamburg, Germany) secondary antibody for 2 hours at room temperature. Visualization was achieved using the enhanced chemiluminescence method (Western Lightning ECL Substrate, Rodgau, Germany) according to manufacturer's protocol. For densitometric quantification, the intensities of the specific bands were scanned and normalized to β -actin bands of the corresponding sample using the Image-ProPlus software (Rockville, MD, USA).

Table 1. Primer sequences.

Primer	Sequence sense 5' - 3'	Anti-sense 5' - 3'
<i>gapdh</i>	ACAACCTTGGCATTGTGGAA	GATGCACGGATGATGTTCTG
<i>il-1β</i>	GAAGAAGAGCCCATCCTCTG	TCATCTCGGAGCCTGTAGTG
<i>FGF-1</i>	TTTATACGGCTCGCAGACAC	GCTTACAGCTCCCGTTCTTC
<i>Mrc-1</i>	TGATTACGAGCAGTGAAGC	GTTACCCGTAAGCCCAATTT
<i>FGF-2</i>	CCAACCGGTACCTTGCTATG	TATGGCCTTCTGTCCAGGTC

<https://doi.org/10.1371/journal.pone.0178622.t001>

Statistical analysis

Results of each animal were averaged and the mean of each experimental group was calculated. All data are given as means \pm SEM. Differences between 2 groups were analyzed by unpaired Student's t-test. De- and remyelination scores were analyzed by nonparametric Kruskal-Wallis test with Dunn multiple comparisons test and Mann-Whitney test (U-test). Statistical analysis was performed using GraphPadPrism 5 (GraphPad software Inc., CA, USA). Statistical significance was set at $p < 0.05$. At least, 4 animals per group were included for gene expression and protein analysis by real-time-PCR and Western blotting, respectively. Cell and myelin quantifications by immunohistochemistry for cuprizone treated or untreated animals and all different control groups mentioned were performed using at least 5 animals per group. The data presented in this study were obtained from 3 independent experiments.

Results

Asm-deficiency enhances myelin recovery after acute and chronic demyelination

In order to investigate the role of *Asm* in demyelination, we treated wild-type and *Asm*-deficient littermate mice with cuprizone for 5 weeks (acute demyelination) or 12 weeks (chronic demyelination), followed by 2 weeks of recovery. The extent of demyelination was assessed immunohistochemically by LFB-PAS staining and myelin basic protein (MBP) staining (Fig 1a). Axonal damage was evaluated by APP and synaptophysin analysis (Fig 2a) in the midline of the corpus callosum (CCm), a brain region characteristically affected in the cuprizone mouse model (Fig 1d). Compared to untreated controls, wild-type mice exposed to 5- or 12-week cuprizone treatment showed a marked reduction of myelin even after the 2-week recovery period. By contrast, myelin formation in the *Asm*-deficient animals was significantly restored after the 2-week recovery phase, following both 5- or 12-week cuprizone treatment (Fig 1b and 1c).

In animals not given a recovery period, the degree of demyelination observed immediately following 5- or 12-week cuprizone treatment did not differ between wild-type and *Asm*-deficient mice (Fig 1b and 1c).

After acute demyelination induced by 5-week cuprizone treatment, a recovery phase resulted in significant reduction of axonal damage in *Asm*-deficient mice compared to wild-type littermates (Fig 2b and 2c). However, axonal injury was not significantly improved in *Asm*-deficient mice compared to wild-type littermates after chronic demyelination (Fig 2b and 2c).

Olig-2 is a cellular oligodendrocyte marker, strongly expressed by oligodendrocyte precursor cells (OPCs) and only weakly by mature oligodendrocytes. [19] Compared to wild-type controls, *Asm*-deficient animals showed a significant increase in oligodendrocyte cell numbers in the CCm than wild-type mice after recovery from both, acute and chronic cuprizone treatment (Fig 3a and 3b).

Myelin growth has been shown to be controlled by fibroblast growth factors (FGF). [20, 21, 22] Therefore, FGF-1 and -2 mRNA levels were analyzed. *Asm*-deficient mice showed a significant increase of FGF-1 and -2 compared to wild-type littermates after the 2-week recovery phase following acute demyelination, hinting towards improved myelin regeneration (Fig 3c and 3d).

Asm-deficiency reduces astrogliosis and production of inflammatory cytokines after acute demyelination

Glial cells, in particular astrocytes, have been discussed to play a dual role in myelin disorders: While they can stabilize synaptic function, they can also promote inflammatory reactions,

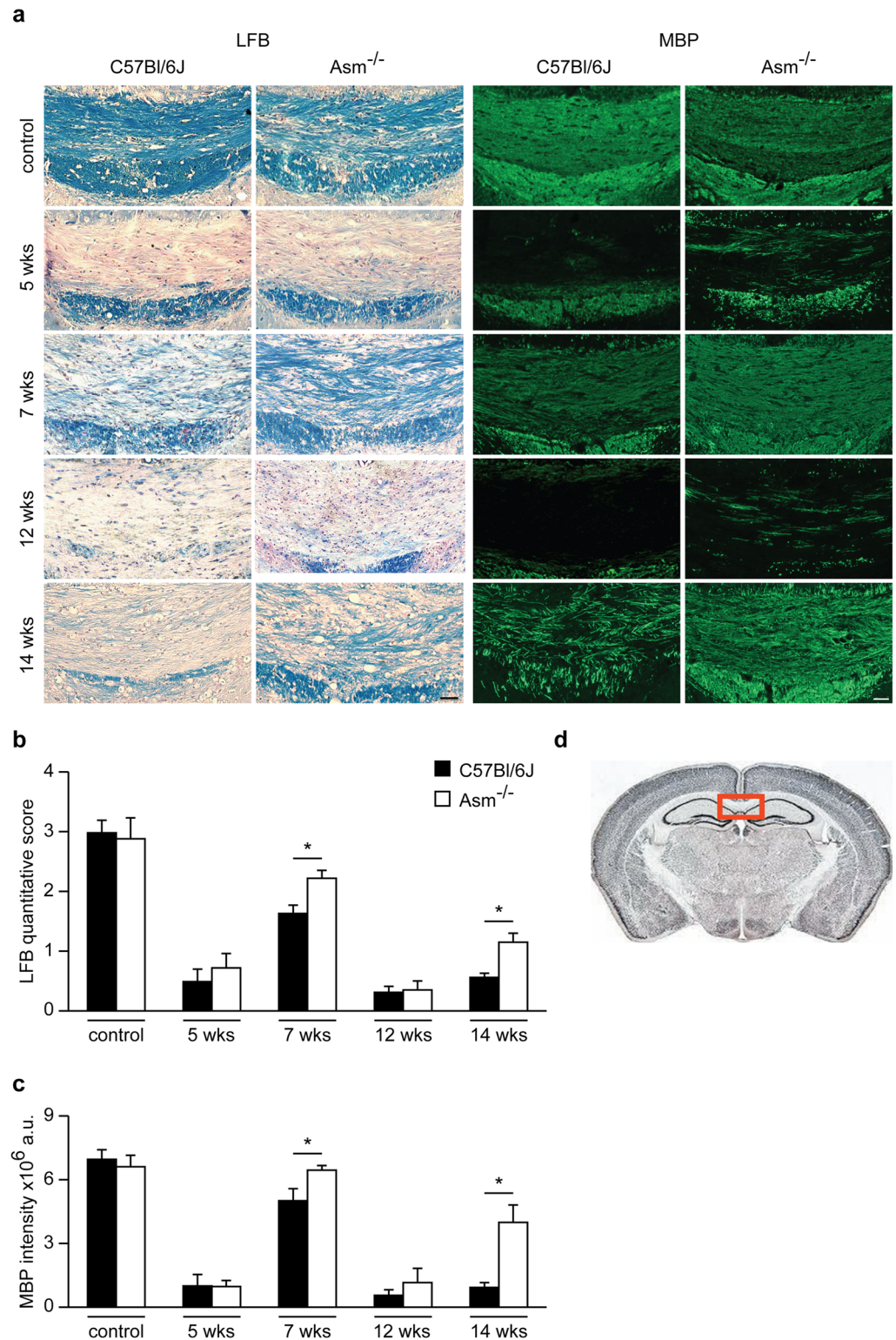


Fig 1. Immunohistochemical staining and quantification of brain sections using LFB and MBP. Cuprizone treatment for 5- or 12-weeks causes a massive decrease in myelination as determined by LFB and MBP staining in the CCm (a). *Asm*-deficient mice showed a significantly increased remyelination compared to wild-type littermates after 2 weeks of recovery following cuprizone treatment as determined by the quantification of myelination score (b) and MBP fluorescence intensity in the CCm (c). Representation of the corpus callosum (d). **p*<0.05 *Asm*-deficient vs wild-type, scale bar: 100 μ m.

<https://doi.org/10.1371/journal.pone.0178622.g001>

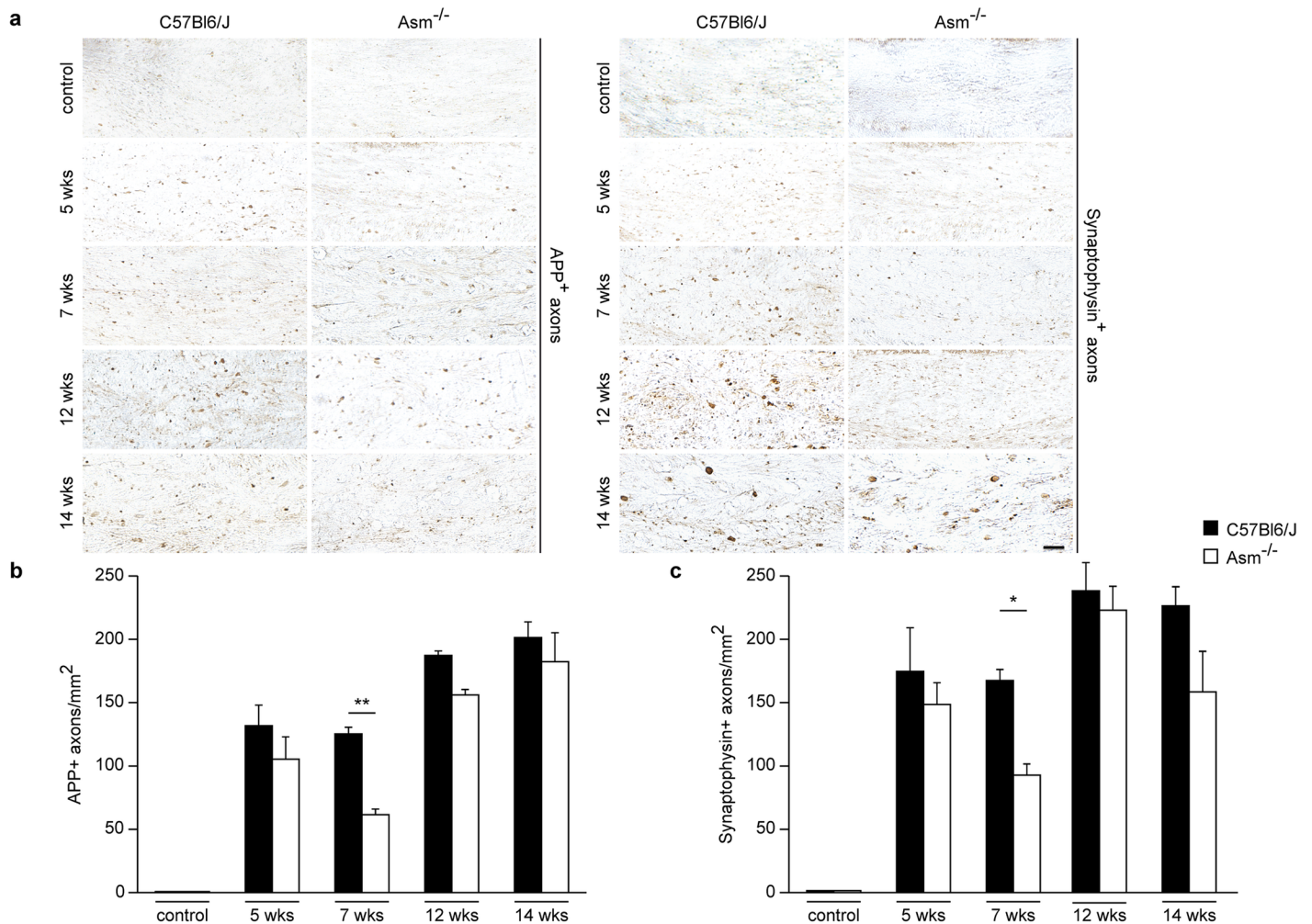


Fig 2. Axonal damage analysis by IHC for APP and synaptophysin. Staining for APP and synaptophysin in the CCm of wild-type and *Asm*-deficient animals after acute or chronic cuprizone treatment followed by 2 weeks recovery period (a). *Asm*-deficient mice showed a significantly lower axonal damage in the 2 weeks recovery phase after acute demyelination (5 weeks cuprizone + 2 weeks recovery) compared to wild-type littermates animals (b and c). However, this difference was not significant after the chronic cuprizone treatment (b and c). ** $p < 0.01$ and * $p < 0.05$ *Asm*-deficient vs wild-types. Scale bar: 100µm.

<https://doi.org/10.1371/journal.pone.0178622.g002>

resulting in myelin and axonal damage. We investigated astroglial and microglial distribution by immunohistochemistry and measured the production of interleukin-1β (IL-1β) and Mrc-1 inflammatory markers by real-time PCR.

GFAP staining intensity revealed a significant reduction in astroglial distribution and astrocytic activation in *Asm*-deficient animals compared to wild-type littermates after the 2-week recovery phase following 5-week cuprizone treatment. This difference was not observed after chronic demyelination (Fig 4a, 4b and 4c). In addition, compared to wild-type littermates, *Asm*-deficient animals showed a significant decrease in pro-inflammatory IL-1β mRNA levels at week 7 (Fig 4d and 4e).

As shown in Fig 5b, 5c and 5d *Asm*-deficient mice showed no difference in microglial distribution nor in mRNA expression of Mrc-1, a marker correlating to anti-inflammatory M2

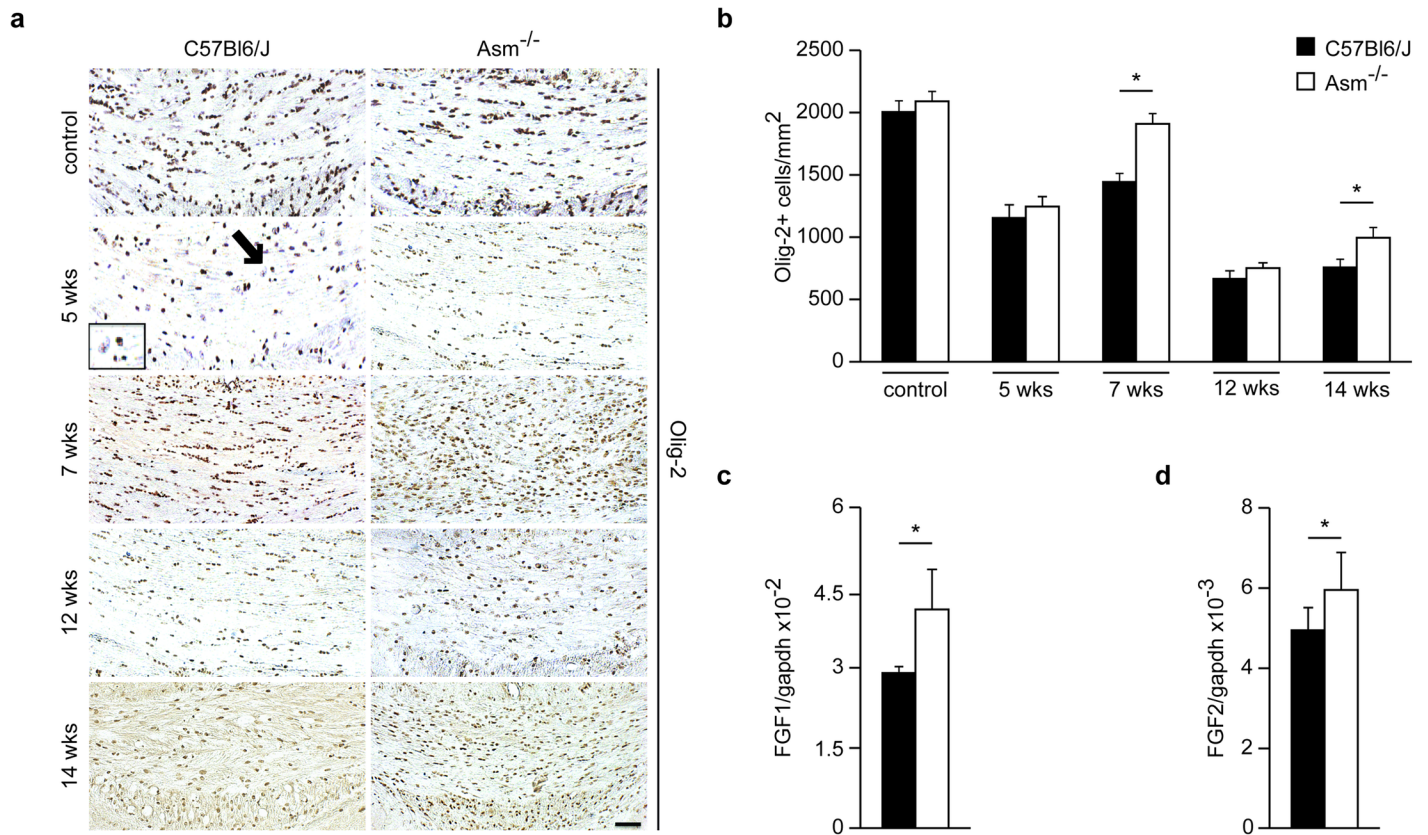


Fig 3. Olig-2 staining for different treatment groups and mRNA analysis of FGF-1 and FGF-2 at week 7. Olig-2⁺ cell numbers were significantly increased in *Asm*-deficient mice compared to wild-type after acute or chronic cuprizone treatment followed by 2 weeks recovery period (a and b). Arrow indicating a strong expression of Olig-2 stain referring to an OPC and nearby a weakly expressed stain by a mature oligodendrocyte. FGF-1 and FGF-2 mRNA levels were also significantly increased after 2 weeks of recovery (week 7) in *Asm*-deficient mice compared to wild-type littermates (c and d). *p<0.05 *Asm*-deficient vs wild-types. Scale bar: 100µm.

<https://doi.org/10.1371/journal.pone.0178622.g003>

microglia phenotype. [23, 24] Glial distribution in the CCm of untreated healthy control mice was quantified (Figs 4 and 5).

Pharmacological inhibition of *Asm* as therapeutic option for myelin repair

To elaborate a potential therapeutic approach, the effect of pharmacological inhibition of *Asm* by amitriptyline [25–26] was investigated in wild-type littermate mice in the acute cuprizone model. Amitriptyline injections or PBS (control) injections were administrated twice daily during the 2-week recovery period following 5-week cuprizone treatment. The intensity of LFB and MBP staining suggested a significantly higher myelin recovery in the CCm of mice with amitriptyline-induced *Asm* inhibition compared to control animals (Fig 6).

Axonal damage in the CCm of animals treated with amitriptyline was significantly lower compared to control-injected mice (Fig 7), as assessed by APP-positive neurons and synaptophysin-positive buds. By contrast, cuprizone-untreated animals did not show any APP- or synaptophysin-positive buds, nor was axonal damage observed (Fig 7b and 7c). After the 2-week recovery period, amitriptyline-treated animals showed higher numbers of olig-2+ cells (Fig 8a and 8b) and higher mRNA levels of the myelin growth factors FGF-1 and -2 (Fig 8c and 8d), compared to control-treated mice. Protein analysis using Western blotting revealed

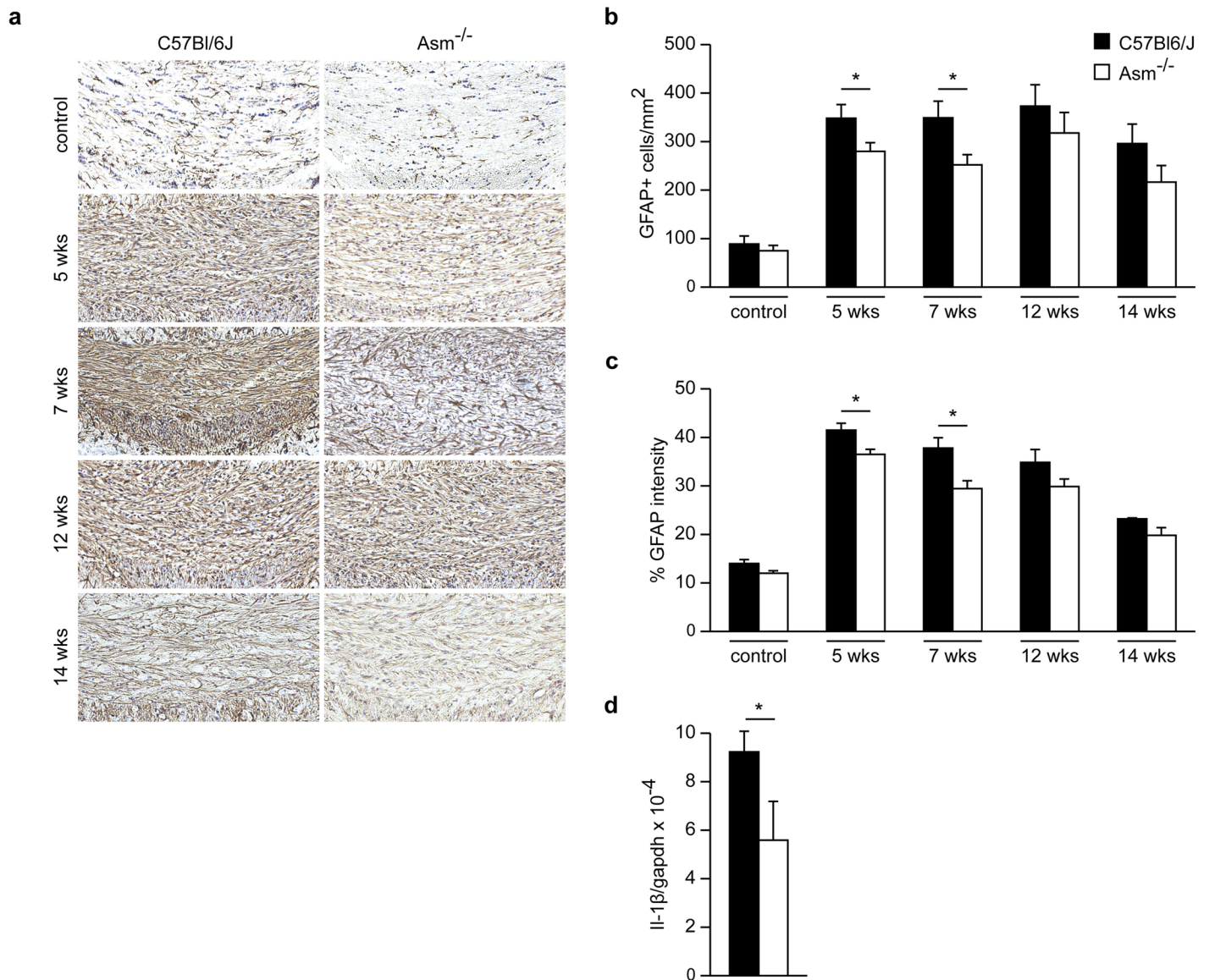


Fig 4. Effect of *Asm*-deficiency on astrogliosis. GFAP stainings in the CCm after 5 or 12 weeks cuprizone treatment followed by 2 weeks remyelination. A significant decrease of astroglial distribution in *Asm*-deficient compared to wild-type littermates after 5 weeks of cuprizone treatment followed by 2 weeks of remyelination was observed (**b and c**). *Asm*-deficiency significantly decreased IL-1β mRNA expression levels compared to wild-type littermates after 5 weeks cuprizone treatment followed by 2 weeks recovery (**d**). * $p < 0.05$ *Asm*-deficient vs wild-type littermates. Scale bar: 100 μm.

<https://doi.org/10.1371/journal.pone.0178622.g004>

higher MOG levels in the CCm of amitriptyline-injected mice compared to control-treated wild-type animals at week 7. Also, *Asm*-deficient animals after 2 weeks of recovery following 5 weeks of cuprizone treatment showed significantly higher levels of MOG compared to wild-type (Fig 8e and 8f).

Asm inhibition by amitriptyline also reduced detrimental astrocytosis compared to control animals. Amitriptyline-treated mice showed a significant reduction in astrocyte cell numbers and GFAP staining intensity in the CCm (Fig 9a, 9b and 9c) as well as significantly lower levels of the inflammatory cytokines IL-1β (Fig 9d). Protein analysis at week 7, revealed a significantly lower level of GFAP in amitriptyline-treated mice compared to control-treated

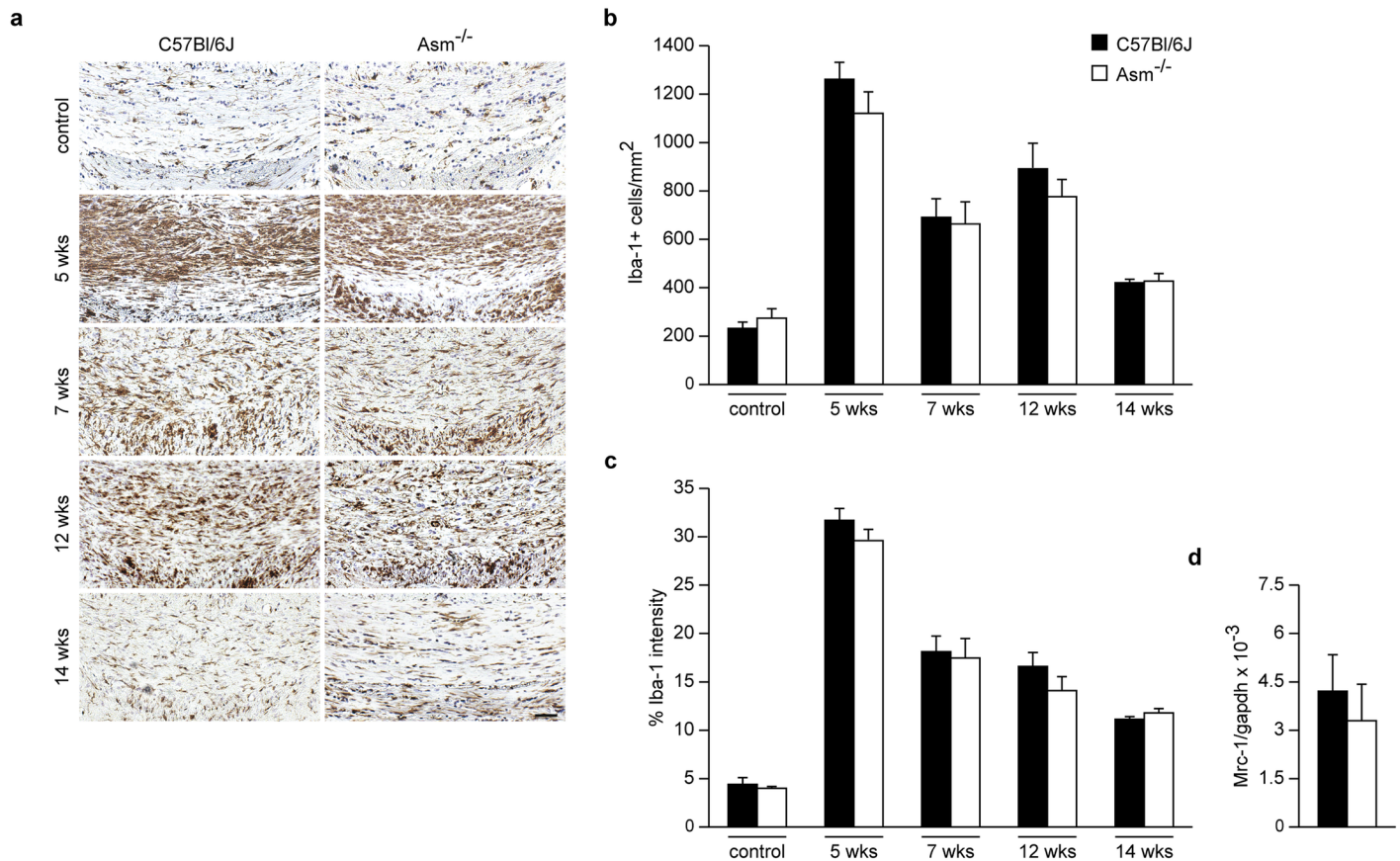


Fig 5. Effect of *Asm*-deficiency on microgliosis and *Mrc-1* mRNA levels. Immunohistochemistry for microglia at different time intervals (a). *Asm*-deficiency had no effect on microgliosis neither in acute nor in chronic groups (b and c). mRNA expression levels of *Mrc-1* showed no significant difference between the compared groups. *Mrc-1* mRNA level expression after 5 weeks demyelination followed by 2 weeks recovery (d) *Asm*-deficient vs wild-type littermates. Scale bar: 100 μ m.

<https://doi.org/10.1371/journal.pone.0178622.g005>

littermates. *Asm*-deficient mice after 5 weeks cuprizone treatment followed by 2 weeks recovery showed significantly reduced GFAP levels compared to wild-type animals (Fig 9e and 9f).

However, amitriptyline-treated and control animals showed no significant differences at week 7 in microglial distribution, including cell number quantification and Iba-1 intensity in the the CCm (Fig 10a, 10b and 10c).

Discussion

Using the cuprizone model, a mouse model used to examine myelin destruction and remyelination in multiple sclerosis, the most common disease of acquired myelin disorders. The results of this study demonstrate that genetic deficiency or pharmacological inhibition of *Asm*/ceramide system can enhance myelin repair after cuprizone-induced demyelination. In our study, deficiency or blockade of the *Asm*/ceramide system significantly improved recovery of myelin, as measured by MBP and LFB intensity scores, and increased oligodendrocyte cell numbers, as indicated by increased Olig-2 positive cells in the recovery phase after cuprizone treatment, leading to a reduction of neuronal damage. *Asm* and its enzymatic product ceramide have been shown to be expressed at higher levels in active human MS lesions compared to unaffected brain tissue. [13, 14]

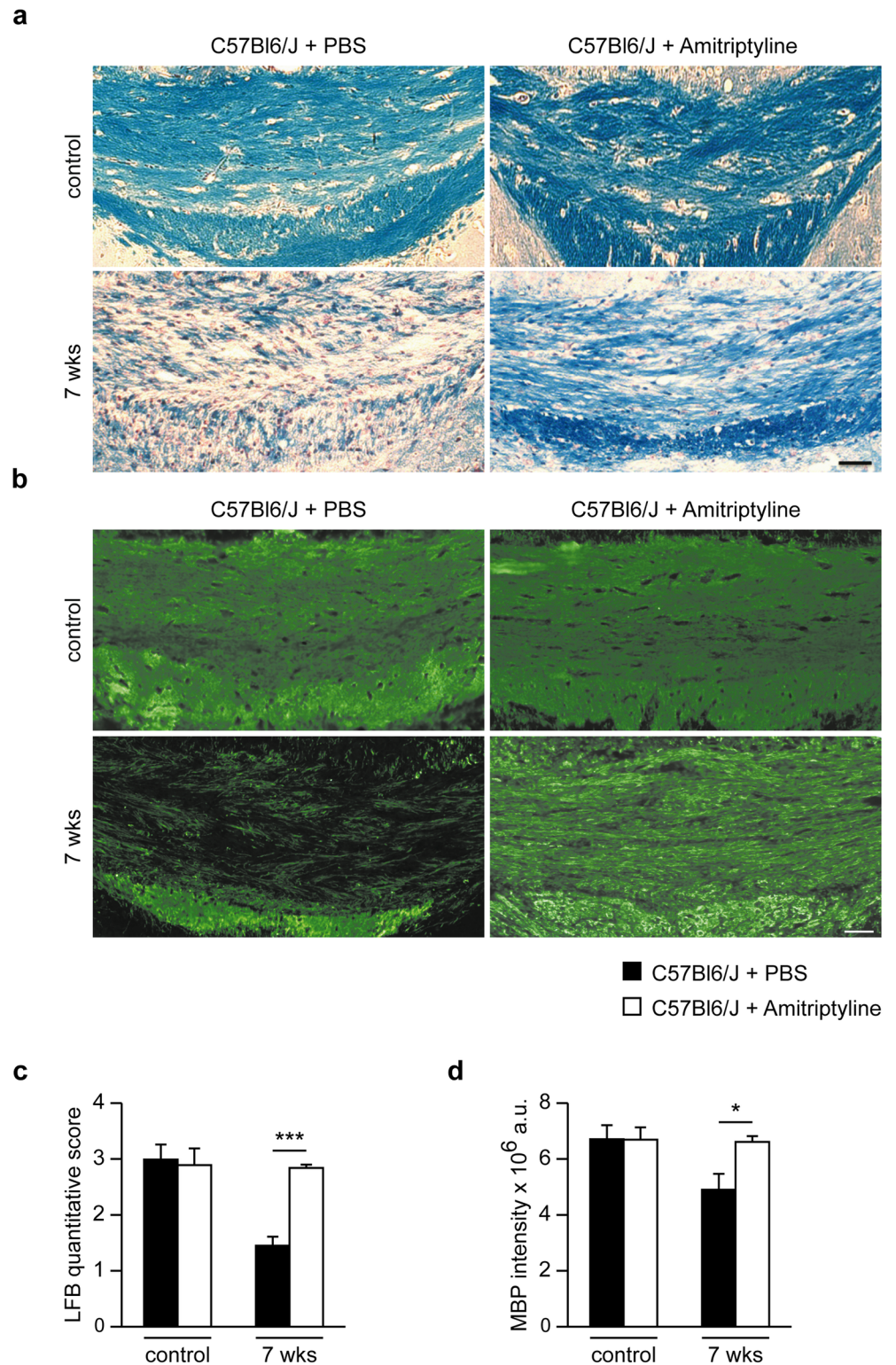


Fig 6. Representative brain sections with CCm stained for LFB and MBP of amitriptyline-treated mice and respective controls. The extent of de- and remyelination was assessed by scoring LFB (a) stained brain section and quantifying MBP (b) intensity of the CCm. The inhibition of Asm by amitriptyline significantly restored myelin compared to control-treated animals after 5 weeks cuprizone treatment followed by 2 weeks of recovery (c and d). ***p<0.001 and *p<0.05 amitriptyline-treated vs control-treated littermates. Scale bar: 100 μ m.

<https://doi.org/10.1371/journal.pone.0178622.g006>

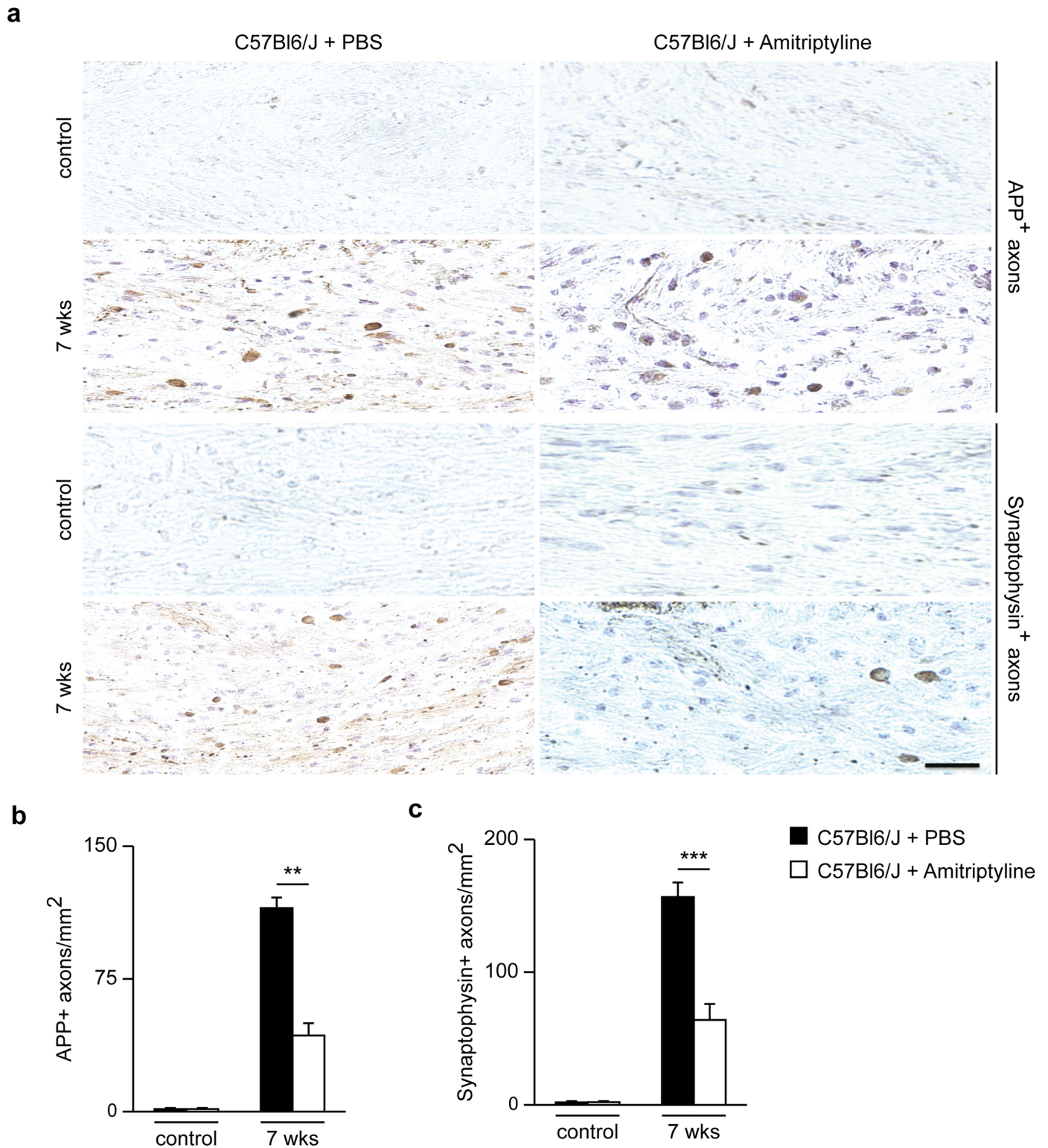


Fig 7. Amyloid precursor protein and synaptophysin detection. Stainings of the CCm of amitriptyline or control-treated animals during the 2 weeks recovery phase after 5 weeks of cuprizone treatment (a). Asm inhibition by amitriptyline showed significantly lower axonal damage, as demonstrated by the quantification of APP and synaptophysin positive buds in the CCm (b, c). ** $p < 0.01$ and *** $p < 0.001$ amitriptyline-treated vs control-treated mice. Scale bar, 50 μ m.

<https://doi.org/10.1371/journal.pone.0178622.g007>

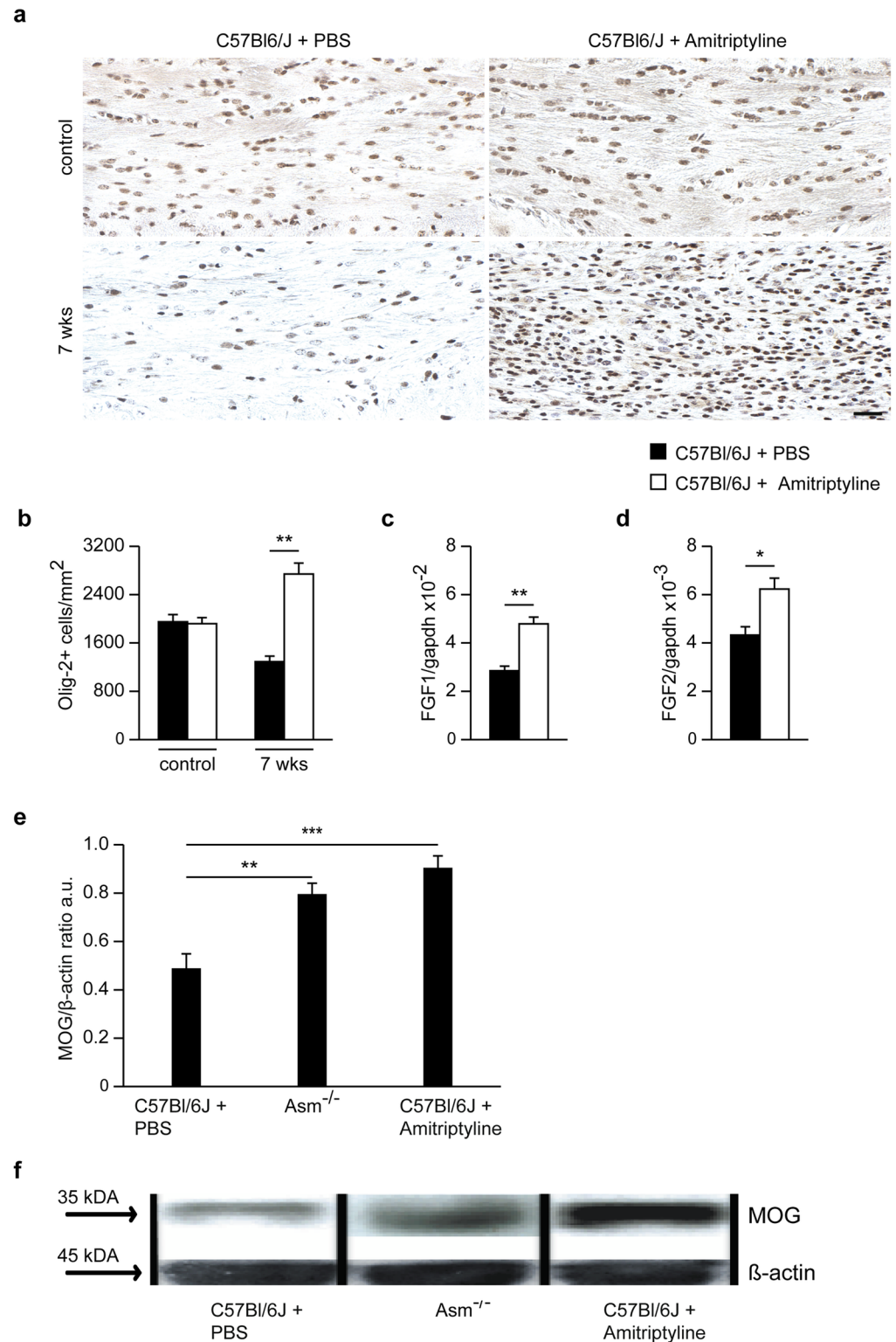


Fig 8. Olig-2 stainings of the CCm of amitriptyline-treated and control treated mice and week 7. Oligodendrocytes in the CCm of amitriptyline-treated mice were significantly increased compared to control-treated animals (**a and b**). mRNA expression levels of the myelin growth factors FGF1 and FGF2 mRNA levels were significantly increased in amitriptyline-treated mice compared to controls (**c and d**). Also, protein levels of MOG were significantly higher in amitriptyline-treated mice compared to control-treated littermates at week 7.

In addition, *Asm*-deficient mice expressed similar MOG levels as amitriptyline-treated mice (e and f). * $p < 0.05$ and ** $p < 0.01$ amitriptyline-treated vs control-treated mice. Scale bar, 50 μm .

<https://doi.org/10.1371/journal.pone.0178622.g008>

Interestingly, MBP/LFB levels and Olig-2 positive cell numbers of amitriptyline-treated animals were close to normal values of untreated mice. This finding is in accordance with the observation that ceramide can act together with the pro-inflammatory cytokine tumor necrosis factor alpha to induce oligodendrocyte cell death in human MS brains. [14] In addition, over expression of *Asm* and subsequent increase of ceramide resulted in reduced neuronal functions even without any further cell stress. [27] Fibroblast growth factors (FGF) are important enhancing factors of myelin growth. [20, 21, 22] Previous studies have shown that FGF blocks *Asm* activation [28], and the beneficial effects of FGF might be, at least in part, mediated by an interaction with the *Asm*/ceramide system. Corroborating this hypothesis is our finding that the myelin growth factors FGF-1 and FGF-2 are significantly increased in the recovery phase after acute demyelination in mice lacking *Asm*, suggesting that the *Asm*/ceramide system negatively regulates FGF after demyelination.

Activation of central nervous system cells, especially astrocytes is hypothesized to be an important mechanism in MS-associated de- and remyelination. [18] Astrocytes can exert a dual role with either beneficial functions (e.g., by facilitating microglial-mediated myelin clearance) [18] or detrimental functions (e.g., by enhancing inflammatory myelin toxic reactions with inflammatory cytokine production). [29]

The significant reduction of activated astrocytes and the decreased levels of IL-1 β mRNA in *Asm*-deficient mice suggest a potential role in myelin repair. Interestingly, enhanced levels of *Asm* mRNA have been described in astrocytes isolated from MS lesions. [13] Although the difference is significant, in our study astrocyte numbers were only 30% reduced in *Asm*-deficient mice compared to wild-type littermates, underscoring the dual beneficial/detrimental role they likely play.

The *Asm*/ceramide system appears to affect the process of remyelination rather than demyelination. Although a significant difference was detected between *Asm*-deficient and wild-type littermates in GFAP at week 5, the differences observed between *Asm*-deficient and wild-type mice were particularly notable in the recovery phase after acute demyelination (5-week cuprizone treatment), suggesting that the involvement of glial cells is critical primarily after acute myelin injury. In contrast, recovery after chronic demyelination (12 weeks of cuprizone) resulted in an increased myelin content and increased oligodendrocyte cell numbers in *Asm*-deficient mice, but did not show a clear glial cell involvement. These results suggest that other mechanisms are likely involved in chronic demyelination.

Microglia have been reported to play a supportive role in remyelination. [29] In the cuprizone animal model, microglial cells increase in number and become activated after cuprizone treatment. [30] Interestingly, in the recovery phase after acute demyelination, *Asm*-deficient mice and their wild-type littermates showed no difference in microglial distribution and activation, excluding any important role of microglia in myelin repair.

The positive effect of *Asm*-deficiency in myelin recovery can be mimicked by treatment with amitriptyline, a well-known pharmacological *Asm* inhibitor [25, 26], suggesting a potential therapeutic approach to support remyelination. In our study, amitriptyline treatment was only initiated after cuprizone-induced myelin damage. Amitriptyline treatment resulted in restoration of MBP and LFB intensity to normal values after 2 weeks, with an even higher than normal level of oligodendrocyte cells. These results strongly suggest a detrimental role of the *Asm*/ceramide system not during myelin damage, but during the repair phase.

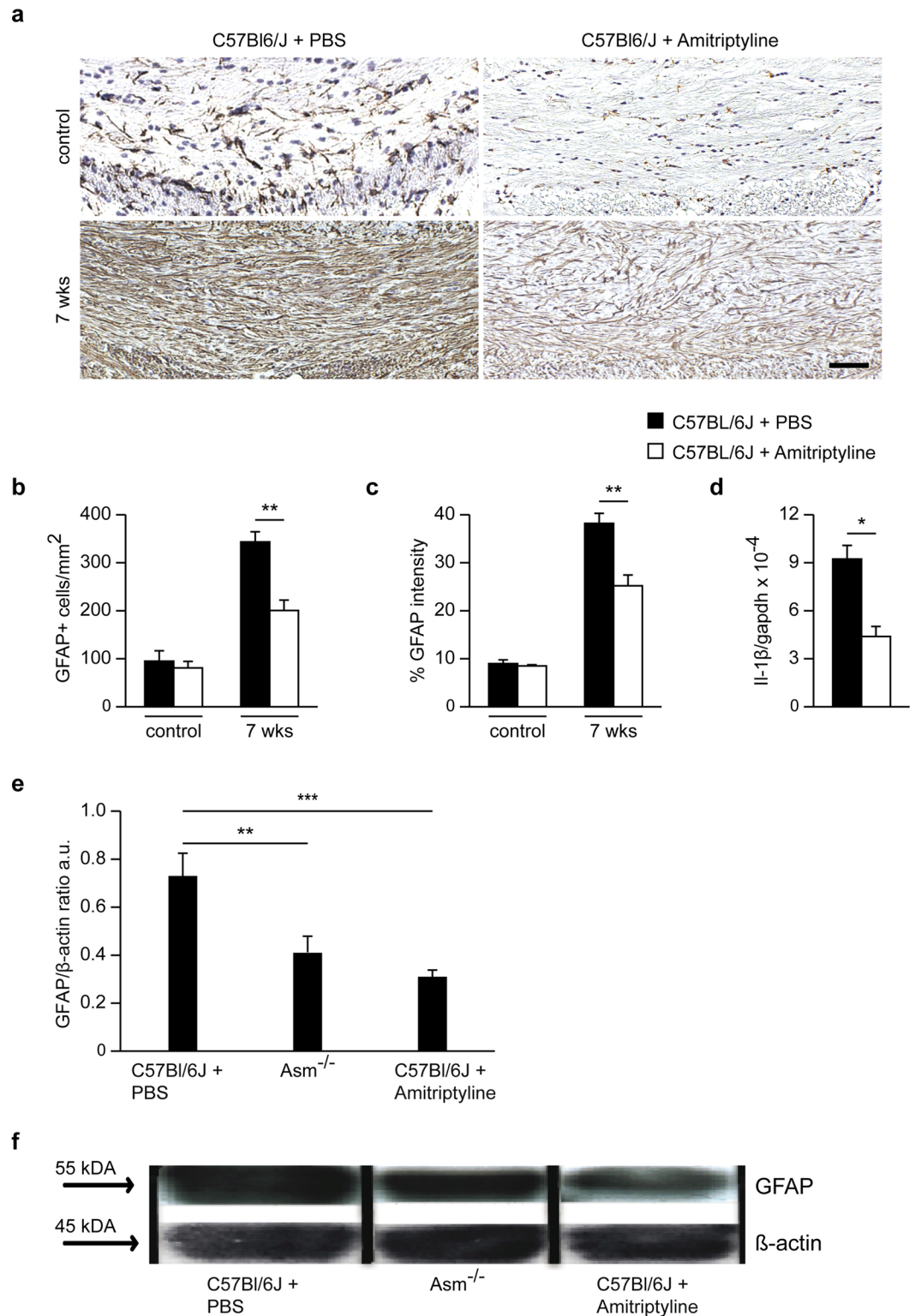


Fig 9. Asm inhibition by amitriptyline for 2 weeks of recovery period after 5 weeks cuprizone feeding effects astrogliosis in the CCm. GFAP⁺ cells and GFAP staining intensity of the CCm significantly decreased in the amitriptyline-treated group compared to control-treated (**b and c**). Asm inhibition by amitriptyline significantly decreased IL-1β mRNA expression (**d**). Western blot analysis revealed that after 2 weeks of recovery with bi-daily amitriptyline-treatment, GFAP protein levels were significantly reduced compared to control-treated littermates. In

addition, *Asm*-deficient mice expressed similar GFAP protein levels as amitriptyline-treated mice (e and f). * $p < 0.05$, ** $p < 0.01$ and *** $p < 0.001$ amitriptyline-treated vs control-treated groups. Scale bar: 100 μm .

<https://doi.org/10.1371/journal.pone.0178622.g009>

Conclusion

In conclusion, we show that the *Asm*/ceramide system is strongly involved in remyelination after acute and chronic myelin damage by reducing astroglia distribution and subsequent pro-inflammatory cytokine release. This might lead to the observed enhanced oligodendrocyte proliferation and neuronal preservation.

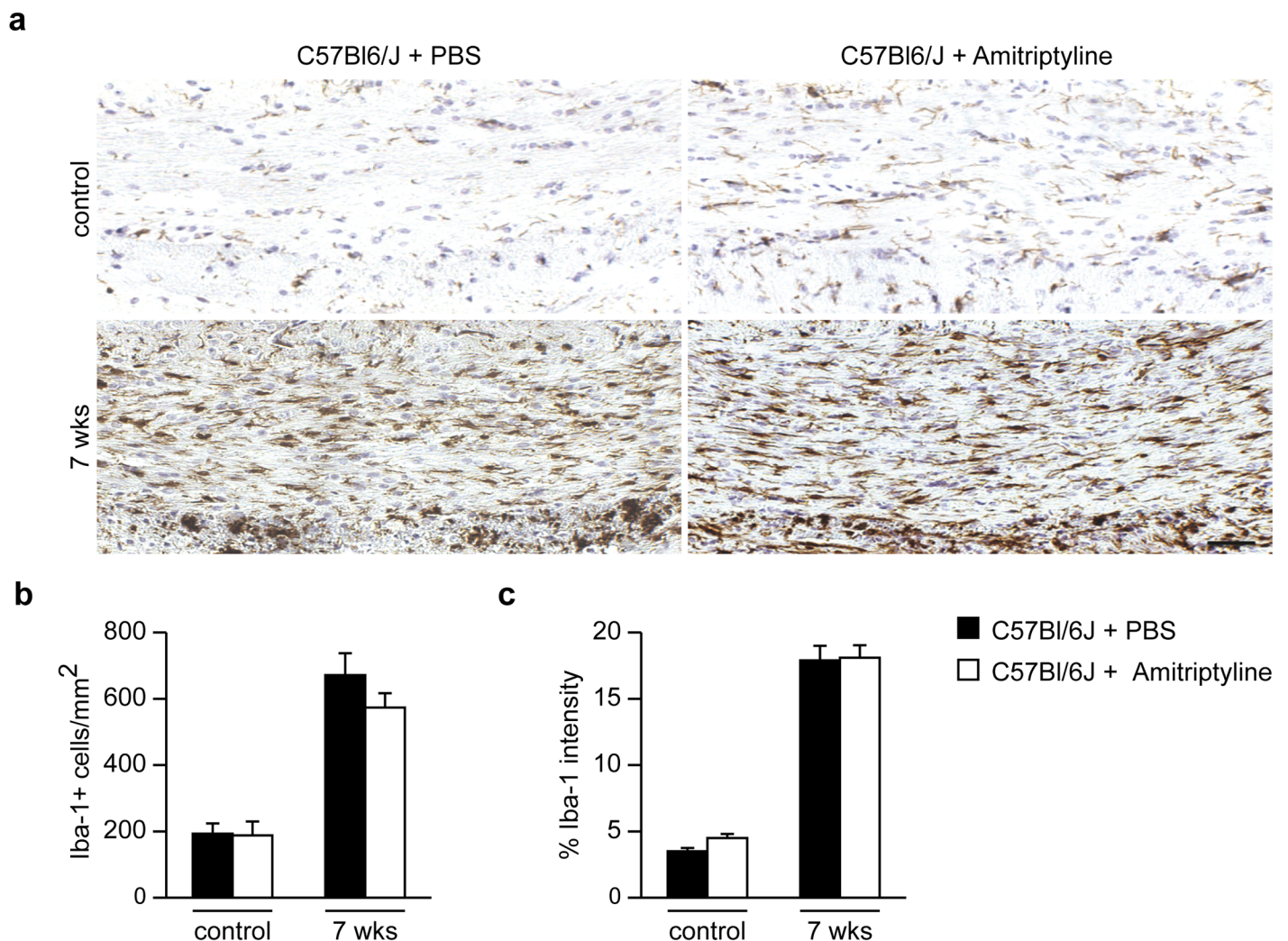


Fig 10. Microglial distribution analysis using Iba-1 staining after *Asm* inhibition by amitriptyline for 2 weeks of recovery period after 5 weeks cuprizone feeding in the CCm. Iba-1⁺ cell numbers and Iba-1 staining intensity in the CCm of amitriptyline- or control-treated animals showed no significance difference (b, c).

<https://doi.org/10.1371/journal.pone.0178622.g010>

Acknowledgments

We would like to express our thanks to Andrea Schottek for excellent technical assistance.

Author Contributions

Conceptualization: RH KB EG KF.

Formal analysis: MC.

Investigation: MC LS.

Methodology: MC.

Project administration: SW.

Supervision: KF SW.

Visualization: RH.

Writing – original draft: SW.

Writing – review & editing: MC RH LS KB CM EG KF.

References

1. Koch-Henriksen N, Sorensen PS. The changing demographic pattern of multiple sclerosis epidemiology. *Lancet Neurol.* 2010; 9(5):520–32. WOS:000277384600016. [https://doi.org/10.1016/S1474-4422\(10\)70064-8](https://doi.org/10.1016/S1474-4422(10)70064-8) PMID: 20398859
2. Fischer MT, Wimmer I, Hoffberger R, Gerlach S, Haider L, Zrzavy T, et al. Disease-specific molecular events in cortical multiple sclerosis lesions. *Brain.* 2013; 136(6):1799–815. <https://doi.org/10.1093/brain/awt110> PMID: 23687122
3. do Carmo Cunha J, de Freitas Azevedo Levy B, de Luca BA, de Andrade MSR, Gomide VC, Chadi G. Responses of reactive astrocytes containing S100 protein and fibroblast growth factor-2 in the border and in the adjacent preserved tissue after a contusion injury of the spinal cord in rats: implications for wound repair and neuroregeneration. *Wound Repair and Regeneration.* 2007; 15(1):134–46. <https://doi.org/10.1111/j.1524-475X.2006.00194.x> PMID: 17244329
4. Zawadzka M, Rivers LE, Fancy SPJ, Zhao C, Tripathi R, Jamen F, et al. CNS-Resident Glial Progenitor/Stem Cells Produce Schwann Cells as well as Oligodendrocytes during Repair of CNS Demyelination. *Cell Stem Cell.* 2010; 6(6):578–90. <https://doi.org/10.1016/j.stem.2010.04.002> PMID: 20569695
5. Wang Y, Cheng X, He Q, Zheng Y, Kim DH, Whittemore SR, et al. Astrocytes from the Contused Spinal Cord Inhibit Oligodendrocyte Differentiation of Adult Oligodendrocyte Precursor Cells by Increasing the Expression of Bone Morphogenetic Proteins. *Journal of Neuroscience.* 2011; 31(16):6053–8. <https://doi.org/10.1523/JNEUROSCI.5524-09.2011> PMID: 21508230
6. Lassmann H. Mechanisms of white matter damage in multiple sclerosis. *Glia.* 2014; 62(11):1816–30. <https://doi.org/10.1002/glia.22597> PMID: 24470325
7. Crawford AH, Stockley JH, Tripathi RB, Richardson WD, Franklin RJM. Oligodendrocyte progenitors: Adult stem cells of the central nervous system? *Experimental Neurology.* 2014; 260:50–5. <https://doi.org/10.1016/j.expneurol.2014.04.027> PMID: 24800913
8. Kipp M, Clarner T, Dang J, Copray S, Beyer C. The cuprizone animal model: new insights into an old story. *Acta Neuropathologica.* 2009; 118(6):723–36. <https://doi.org/10.1007/s00401-009-0591-3> PMID: 19763593
9. Schneider PB, Kennedy EP. Sphingomyelinase in Normal Human Spleens and in Spleens from Subjects with Niemann-Pick Disease. *Journal of Lipid Research.* 1967; 8(3):202–+. WOS: A19679278500007. PMID: 4962590
10. Grassmé H, Jekle A, Riehle A, Schwarz H, Berger J, Sandhoff K, et al. CD95 Signaling via Ceramide-rich Membrane Rafts. *Journal of Biological Chemistry.* 2001; 276(23):20589–96. <https://doi.org/10.1074/jbc.M101207200> PMID: 11279185
11. Gulbins E. Regulation of death receptor signaling and apoptosis by ceramide. *Pharmacological Research.* 2003; 47(5):393–9. [https://doi.org/10.1016/s1043-6618\(03\)00052-5](https://doi.org/10.1016/s1043-6618(03)00052-5) PMID: 12676513

12. Marchesini N, Hannun YA. Acid and neutral sphingomyelinases: roles and mechanisms of regulation. *Biochemistry and Cell Biology*. 2004; 82(1):27–44. <https://doi.org/10.1139/o03-091> PMID: 15052326
13. van Doorn R, Nijland PG, Dekker N, Witte ME, Lopes-Pinheiro MA, van het Hof B, et al. Fingolimod attenuates ceramide-induced blood–brain barrier dysfunction in multiple sclerosis by targeting reactive astrocytes. *Acta Neuropathologica*. 2012; 124(3):397–410. <https://doi.org/10.1007/s00401-012-1014-4> PMID: 22810490
14. Kim S, Steelman AJ, Zhang Y, Kinney HC, Li J. Aberrant Upregulation of Astroglial Ceramide Potentiates Oligodendrocyte Injury. *Brain Pathology*. 2012; 22(1):41–57. <https://doi.org/10.1111/j.1750-3639.2011.00501.x> PMID: 21615590
15. Teichgräber V, Ulrich M, Endlich N, Riethmüller J, Wilker B, De Oliveira–Munding CC, et al. Ceramide accumulation mediates inflammation, cell death and infection susceptibility in cystic fibrosis. *Nature Medicine*. 2008; 14(4):382–91. <https://doi.org/10.1038/nm1748> PMID: 18376404
16. Paxinos G and Franklin KBJ. *The mouse brain in stereotaxic coordinates*. Academic press. 2001; 2(2).
17. Zendedel A, Kashani IR, Azimzadeh M, Pasbakhsh P, Omid N, Golestani A, et al. Regulatory effect of triiodothyronine on brain myelination and astrogliosis after cuprizone-induced demyelination in mice. *Metabolic Brain Disease*. 2016; 31(2):425–33. <https://doi.org/10.1007/s11011-015-9781-y> PMID: 26725831
18. Skripuletz T, Hackstette D, Bauer K, Gudi V, Pul R, Voss E, et al. Astrocytes regulate myelin clearance through recruitment of microglia during cuprizone-induced demyelination. *Brain*. 2012; 136(1):147–67. <https://doi.org/10.1093/brain/aws262> PMID: 23266461
19. Kuhlmann T, Lassmann H, Brück W. Diagnosis of inflammatory demyelination in biopsy specimens: a practical approach. *Acta Neuropathologica*. 2008; 115(3):275–87. <https://doi.org/10.1007/s00401-007-0320-8> PMID: 18175128
20. Messersmith DJ, Murtie JC, Le TQ, Frost EE, Armstrong RC. Fibroblast growth factor 2 (FGF2) and FGF receptor expression in an experimental demyelinating disease with extensive remyelination. *J Neurosci Res*. 2000; 62(2):241–56. [https://doi.org/10.1002/1097-4547\(20001015\)62:2<241::AID-JNR9>3.0.CO;2-D](https://doi.org/10.1002/1097-4547(20001015)62:2<241::AID-JNR9>3.0.CO;2-D) WOS:000089702300009. PMID: 11020217
21. Furusho M, Dupree JL, Nave KA, Bansal R. Fibroblast Growth Factor Receptor Signaling in Oligodendrocytes Regulates Myelin Sheath Thickness. *Journal of Neuroscience*. 2012; 32(19):6631–41. <https://doi.org/10.1523/JNEUROSCI.6005-11.2012> PMID: 22573685
22. Mohan H, Friese A, Albrecht S, Krumbholz M, Elliott CL, Arthur A, et al. Transcript profiling of different types of multiple sclerosis lesions yields FGF1 as a promoter of remyelination. *Acta Neuropathologica Communications*. 2014; 2(1). <https://doi.org/10.1186/s40478-014-0168-9> PMID: 25589163
23. Colton CA, Mott RT, Sharpe H, Xu Q, Van Nostrand WE, Vitek MP. Expression profiles for macrophage alternative activation genes in AD and in mouse models of AD. *Journal of Neuroinflammation*. 2006; 3(1):27. <https://doi.org/10.1186/1742-2094-3-27> PMID: 17005052
24. Röszer T. Understanding the Mysterious M2 Macrophage through Activation Markers and Effector Mechanisms. *Mediators of Inflammation*. 2015; 2015:1–16. <https://doi.org/10.1155/2015/816460> PMID: 26089604
25. Kornhuber J, Tripal P, Reichel M, Muhle C, Rhein C, Muehlbacher M, et al. Functional Inhibitors of Acid Sphingomyelinase (FIASMA)s: A Novel Pharmacological Group of Drugs with Broad Clinical Applications. *Cell Physiol Biochem*. 2010; 26(1):9–20. <https://doi.org/10.1159/000315101> WOS:000277890300002. PMID: 20502000
26. Kornhuber J, Muehlbacher M, Trapp S, Pechmann S, Friedl A, Reichel M, et al. Identification of Novel Functional Inhibitors of Acid Sphingomyelinase. *PLoS ONE*. 2011; 6(8):e23852. <https://doi.org/10.1371/journal.pone.0023852> PMID: 21909365
27. Gulbins E, Palmada M, Reichel M, Lüth A, Böhmer C, Amato D, et al. Acid sphingomyelinase–ceramide system mediates effects of antidepressant drugs. *Nature Medicine*. 2013; 19(7):934–8. <https://doi.org/10.1038/nm.3214> PMID: 23770692
28. Jacobi J, García-Barros M, Rao S, Rotolo JA, Thompson C, Mizrahi A, et al. Targeting acid sphingomyelinase with anti-angiogenic chemotherapy. *Cellular Signalling*. 2016; 29:52–61. <https://doi.org/10.1016/j.cellsig.2016.09.010> PMID: 27702691
29. Gudi V, Gingele S, Skripuletz T, Stangel M. Glial response during cuprizone-induced de- and remyelination in the CNS: lessons learned. *Frontiers in Cellular Neuroscience*. 2014; 8. <https://doi.org/10.3389/fncel.2014.00073> PMID: 24659953
30. Goldberg J, Clarner T, Beyer C, Kipp M. Anatomical Distribution of Cuprizone-Induced Lesions in C57BL6 Mice. *Journal of Molecular Neuroscience*. 2015; 57(2):166–75. <https://doi.org/10.1007/s12031-015-0595-5> PMID: 26067430